Whey protein fluid gels for the stabilisation of foams

Lazidis, A.; Hancocks, Robin; Spyropoulos, F.; Kreuß, M.; Berrocal, R.; Norton, Ian

DOI:
10.1016/j.foodhyd.2015.02.022

Accepted Manuscript

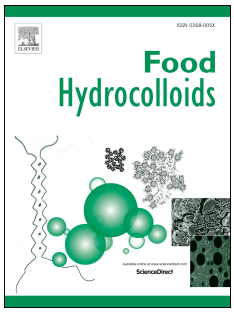

Whey Protein Fluid Gels for the stabilisation of foams

A. Lazidis, R.D. Hancocks, F. Spyropoulos, M. Kreuß, R. Berrocal, I.T. Norton

PII: S0268-005X(15)00083-1

DOI: 10.1016/j.foodhyd.2015.02.022

Reference: FOOHYD 2897

To appear in: *Food Hydrocolloids*

Received Date: 10 November 2014

Revised Date: 10 February 2015

Accepted Date: 17 February 2015

Please cite this article as: Lazidis, A., Hancocks, R.D., Spyropoulos, F., Kreuß, M., Berrocal, R., Norton, I.T., Whey Protein Fluid Gels for the stabilisation of foams, *Food Hydrocolloids* (2015), doi: 10.1016/j.foodhyd.2015.02.022.

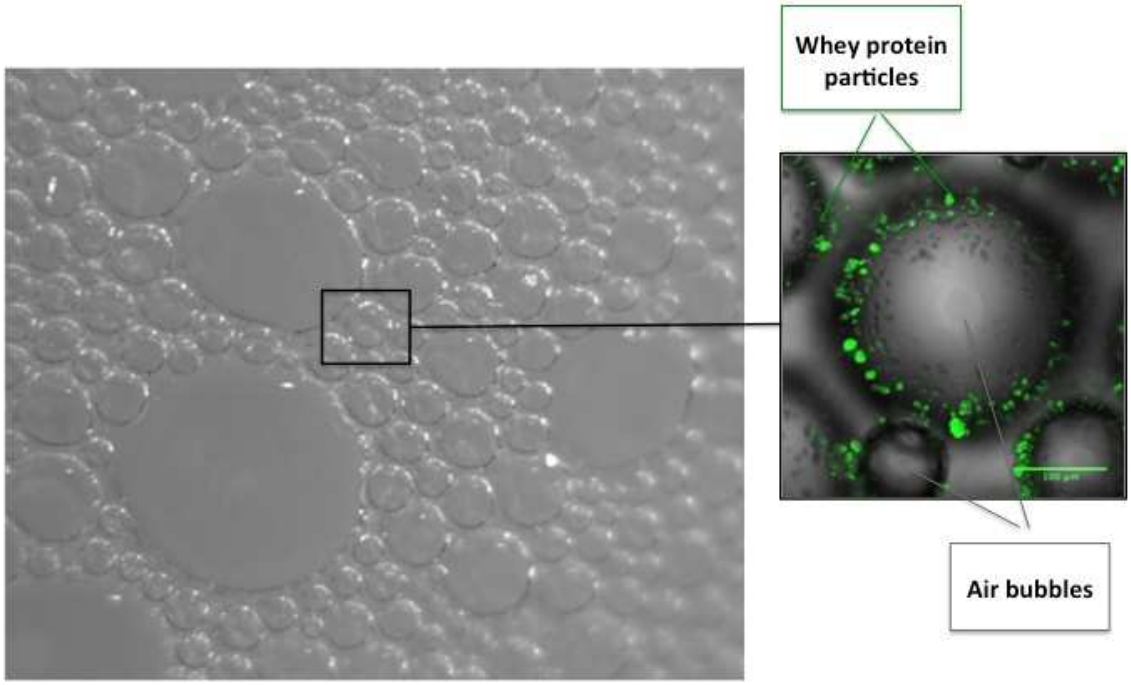

Whey Protein Fluid Gels for the stabilisation of foams

A. Lazidis[a,□], R.D. Hancocks[a], F. Spyropoulos[a], M. Kreuß[b], R. Berrocal[b], I.T. Norton[a]

[a]*Chemical Engineering Department, University of Birmingham, Edgbaston B15 2TT, UK*

[b]*Nestlé Product Technology Centre, 3510 Konolfingen, Switzerland*

□Corresponding author. Email address: axl176@bham.ac.uk□□

Abstract

The ability of whey protein fluid gels to produce very stable foams was demonstrated. These systems were prepared by heat induced gelation within the turbulent flow field of a pin stirrer at pH 5 and 8. The effect of pH and final protein concentration on the morphology of the particles, the bulk, interfacial and rheological properties and finally the foaming properties of their aqueous suspensions were investigated. Whey protein fluid gels, when produced close to the isoelectric point, consist of small spherical protein aggregates without significant functionality. Micrographs taken suggest that the protein aggregates created have the ability to adsorb at the air/water interface. Nevertheless, the lack of further increase in interfacial viscosity or elasticity indicates that either the adsorption is easily reversible or that it is only partial due to lack of material available to provide complete coverage. By increasing the pH of these systems the protein entities present acquire a negative charge, which causes an increase to both the bulk and interfacial viscoelasticity and increase of the stability of foams. The proposed mechanism is that during foaming, the smaller and mobile protein entities diffuse fast to the interface and provide the necessary interfacial tension reduction to facilitate foam formation. Subsequently, the larger protein particles fill the free space between the air bubbles and increase the local bulk viscosity, which improves foam stability mainly by preventing drainage. Whey protein fluid gels were able to create the same amount of foam as non-treated whey proteins but with substantially increased stability.

1 Introduction

Aeration of foods is a process that is used both in traditional food products like bread and whipped cream but also in contemporary ones such as aerated chocolate, hot beverages and gourmet dishes. The presence of air, usually in the form of bubbles, throughout the volume of food provides a unique texture, which is frequently associated with luxury and high quality. Furthermore, when aeration is used effectively it can reduce the caloric value and the cost of foods by introducing an ingredient that costs nothing and has no nutritional value.

Aerated materials where the gas, in most cases atmospheric air, is distributed throughout an aqueous continuous phase are colloidal dispersions known as foams. These are thermodynamically unstable systems that generally have significantly shorter lifetime when compared to other colloidal dispersions such as emulsions (hours or even minutes compared to months) (Walstra, 2003). The main reason for the high instability lies to the fact that the interface between the dispersed and continuous phase, also called film, is larger in size when looking at bubbles in contrast to emulsion droplets. Moreover, the interfacial tension on the air-water interface (surface tension) is larger compared to the one between oil and water by a factor of 5 (Dickinson, 2010). The main mechanisms responsible for destabilising foams are drainage, disproportionation (the equivalent of Ostwald ripening in emulsions) and coalescence (Kinsella, 1981). In practice, these mechanisms reinforce each other commencing a snowball effect towards the breakdown of the foam structure. For instance, the larger bubbles formed due to disproportionation increase the size of the films which accelerate drainage and escalate instability (Walstra, 2003).

Foams are stabilised by amphiphilic entities, which can adsorb at the air/water interface and reduce the surface tension. Food foams are usually stabilised by high molecular weight surfactants or particles. Milk and egg proteins are very common ingredients present in foods that contain bubbles. Particle stabilised foams on the other hand are only present in whipped cream and ice cream where the foam structure is stabilised by a particulate matrix of either partially coalesced fat or ice crystals or both (Dickinson & Murray, 2006). Particles have shown an increased potential in producing ultra stable foams but in most of the cases the material used is non food (Eric Dickinson, 2010). Trying to fulfil this need for finding food grade materials than can produce particles with foam stabilising properties, several studies have focused on plant carbohydrate materials (starches and cellulose derivatives) in combination with surfactants like proteins. These systems have demonstrated potential (Murray, Durga, Yusoff, & Stoyanov, 2011). Particles present in foams can provide stability whether they adsorb on the interface or remain on the continuous phase. In case of adsorption, they form rigid films that are stable against drainage and disproportionation, which is evident from an increase of the interfacial elasticity and viscosity. When there is no adsorption the particles either go through a percolation process and create a gel-like network or act as corks reducing the drainage of the continuous phase due to gravity (Rullier, Novales, & Axelos, 2008).

As the recent consumer trend demands foods to be 'natural' and 'wholesome' accompanied by a 'clean label', there is a need of producing particles from readily available food ingredients (Brockman & Beeren, 2011). A solution lies on the ability of several proteins to produce aggregates and gels when a set of conditions are met. In this study the heat denaturation of whey proteins is being explored as a mechanism to create micron sized aggregates or gel particles that will entail the necessary surface

properties to adsorb on the air/water interface and produce very stable foams. Similar systems containing discrete gel protein particles created by freeze drying quiescently gelled whey protein isolate (WPI) suspensions prepared at a range of pH (5 to 8) has shown prominent results (Lazidis et al., 2014). The whey protein gel particles when rehydrated were able to produce foams with an increased stability by up to an order of magnitude compared to native proteins at the same concentration. That method allowed a significant proportion of whey proteins to remain in their native form and potentially in a form of soluble aggregates. It has been demonstrated in the past that the foaming properties of mixtures of soluble proteins with insoluble aggregates have enhanced foaming properties (Zhu & Damodaran, 1994).

This study focuses on exploring a process of producing gel micro particles that has a potential in future upscaling for manufacture through an industrially applicable process. The ultimate goal is to produce micro particle suspensions that will be in a state which will allow transport through a pump to a drying operation in order to achieve a powder formulation. The route chosen was the implementation of the well established method of producing fluid gels by subjecting a polymer solution to gelling conditions (pH, ionic strength, concentration, temperature) while being under a shear field (Norton, Jarvis, & Foster, 1999). In this case WPI solutions were heated at the critical gelation temperature while subjecting them to the turbulent flow field of a pin stirrer device. In this context, the effect of processing conditions (heating and mixing rate) along with the effect of environmental conditions (pH) on the physicochemical characteristics and foaming properties of the WPI gel particulates were assessed.

2 Materials and methods

2.1 Manufacture of WPI Fluid Gels

WPI BiPRo (Davisco, MN, US) suspensions were prepared at 12 wt% protein concentration using reverse osmosis (RO) water and 0.001 wt% sodium azide (NaN_3) (Sigma Aldrich, Dorset, UK) to prevent microbiological growth. The suspensions were left stirring overnight at 4 ºC to fully hydrate. The pH of the solutions was then adjusted to the desired value using 5M NaOH or 5M HCl (Sigma Aldricht, Dorset, UK). For creating the fluid gels the solutions were pre-heated to 40 ºC and then fed through a peristaltic pump to a series of two jacketed pin stirrers of well defined geometries (Gabriele, 2011). The first pin stirrer device was set to 80 ºC and 2000 rpm rotation speed. The speed of the feed pump was adjusted in order to provide a retention time inside the pin stirrer corresponding to a heating rate of 2 ºC min^{-1}. The outlet of the first pin stirrer was connected to an identical second pin stirrer rotating at 2000 rpm and set to a temperature of 5 ºC that was used for cooling and diluting the primary fluid gel. For diluting the primary fluid gel RO water at room temperature (25 ºC) was fed through a second inlet of the second pin stirrer at a rate that would allow the final dilution of the initial 12 wt% to 5, 3 and 1 wt% which represented more relevant concentrations to the study of foaming. The final fluid gel was stored in glass bottles at 4 ºC until further characterisation.

2.2 Preparation of foams and determination of foam stability

Foams were prepared with two different methods, gas sparging and mechanical whipping. When foam stability and rate of drainage was assessed, foams were prepared by bubbling using a method adapted from literature (Waniska & Kinsella, 1979). Foam was created inside a clear acrylic circular column (75 mm internal diameter and 500 mm in height) by air sparging at a rate of 3 l min^{-1} and pressure of 2 bars through the bottom of the column where a porosity 3 (15 – 40 μm pores) glass sintered plate is located. A

sample of 150 ml suspension was placed in the column and then air sparging was initialised until the production of a foam head of 20 cm. The reduction of the height of the foam head was then recorded with a CCD camera and the foam half-life was later calculated. All measurements were carried out in four replicates.

For all other measurements, foams were produced by mechanical whipping using a commercial milk frother with a spiral impeller of 10 mm diameter rotating at approximately 2000 rpm. For the means of foam production, 20 ml of sample was placed in a 100 ml glass beaker and whipped for 30 seconds. All measurements were performed at 25 ºC unless otherwise stated.

2.3 Determination of foam overrun

The foaming ability of the systems studied was investigated by measuring the amount of air that was able to be incorporated after foaming by mechanical whipping. This was done by weighing equal volumes of the original dispersion and the corresponding foam and calculating the overrun through Eq. 1. The experiments were repeated in a set of five replicates.

$$\%\, overrun = \frac{m_{dispersion} - m_{foam}}{m_{foam}} \times 100 \quad \textbf{(1)}$$

2.4 Determination of foam drainage from conductivity data

A conductivity column was developed in house based on the concept from (Barigou, Deshpande, & Wiggers, 2001) where the conductivity was measured at different heights of the foam across the side and the centre of the column. Alternating current (AC) in a square waveform with a frequency of 1 kHz and a max voltage of 10 volts was fed through the volume of the foam and the drop of the root mean square value of the AC voltage (AC_{RMS}) was monitored. A calibration curve (Figure 1) of different AC_{RMS} values

of known liquid fractions of a foam were plotted and a two parameter logarithmic equation was fitted which was used to calculate the volume of liquid of foams according to equation 2.

$$AC_{RMS} = 2.609 \times \ln V_{liq} - 2.806 \quad (2)$$

Where V_{liq} is the volume of the liquid in the foam and AC_{RMS} is the voltage square mean reading through the whole volume of the foam.

2.5 Measurement of particle size

The particle size distributions of the gel particles present in the fluid gels were determined by laser diffraction after dispersing the powders in water at a concentration of 0.25 wt% and using a Malvern Mastersizer 2000 with a Hydro SM manual small volume dispersion unit attached (Malvern Instruments, UK). The scattered intensity as a function of the angle was transformed into size distribution using the Mie theory and the relevant refractive index for the protein (1.456) was used. All size measurements were carried out in three replicates.

2.6 Determination of ζ-potential

The ζ-potential was determined using a Zetasizer (Malvern Instruments, UK) equipped with an automatic titration unit that allowed the determination of ζ-potential over a wide range of pH (2-12). The titrator used NaOH and HCl of 0.5 and 1M to increase and decrease the pH accordingly.

2.7 Characterisation of rheological properties of the fluid gels

Viscosity and rheological measurements were performed using a Kinexus rheometer (Malvern, UK). Flow curves of the WPI fluid gels were obtained by using roughened

parallel plates with a diameter of 60 mm and applying a range of shear rates (0.01 – 100 s^{-1}) while measuring the viscosity.

The rheological properties of the bulk phase were determined by oscillatory rheology by applying a strain controlled frequency sweep at a strain rate within the linear viscoelastic region of the samples as defined by an amplitude sweep performed beforehand using a similar sample. The oscillations were performed using the same parallel plate geometry. All rheological measurements were carried out in three replicates.

2.8 Surface tension measurements

The Wilhelmy plate method was used to measure the static surface tension of the solution using a K100 Tensiometer from Kruss GmbH (Hamburg, Germany). The plate was allowed to equilibrate for 1200 s while the surface tension was being recorded. All measurements were carried out in three replicates..

2.9 Interfacial dilational rheology

The dynamic air/water (a/w) surface elasticity and viscosity were measured using a pendant-drop Sinterface PAT1 tensiometer (Sinterface, Berlin, Germany). A droplet of the liquid sample with an area of 20 mm^2 was formed automatically at the tip of a syringe driven by a motor plunger within a thermostatically controlled glass cuvette set to 20 ± 0.5 ºC. The image of the drop was captured and digitised by a CCD camera. The interfacial tension ($\sigma_{a/w}$) was calculated by analysing the profile of the drop and fitting it to the Laplace equation. After allowing 1000 s to reach equilibrium sinusoidal oscillations of the interface occurred by injecting and extracting volume into and from the drop while the response in interfacial tension was recorded. The relative amplitude ($\Delta A/A$) of the oscillations was set to 5% in order to stay within the linear viscoelastic region and the

frequency ranged from 0.01 to 0.2 Hz while 0.01 Hz was the frequency chosen as the one relevant to foams (Schmitt, Bovay, & Rouvet, 2014). The dilatational parameters were calculated through a Fourier transformation algorithm implemented in the software package. The dilatational elasticity and viscosity were calculated from equations 3 and 4.

$$|E| = A \times \frac{\Delta\sigma_{a/w}}{\Delta A} = E' + iE'' \quad (3)$$

$$\eta_d = \frac{E''}{\omega} \quad (4)$$

where A is the area of the drop (mm^2), $\sigma_{a/w}$ the air/water interfacial tension (mN m^{-1}), E' the dilatational elasticity (mN m^{-1}), E'' *the loss dilatational modulus (*mN m^{-1}), η_d the dilatational viscosity (mN s m^{-1}) and ω the frequency (Hz). All experiments were duplicated.

2.10 Imaging microstructure by confocal laser scanning microscopy (CLSM)

The microstructure of the protein gel particles in the foams were visualised at 20 ℃ using a confocal scanning laser microscope Leica TCS SPE (Heidelberg, Germany) equipped with laser operating at a wavelength of 532 nm. The WPI fluid gel particles were stained with 0.01 wt% rhodamine B (Sigma Aldricht, Dorset, UK) that was diluted in the protein suspensions prior to the fluid gel manufacturing.

2.11 Statistical analysis

All the data of the replicated measurements of the study that are plotted in the present publication include the average of the measurement accompanied by error bars that consist of the standard deviation (SD) of the mean. In the case where mean values of an observation are compared between samples the data have been subjected to

analysis of variance (one-way ANOVA) in order to determine significant differences between the samples. Data where checked for following normal distribution and equality of variance prior to carrying out the ANOVA. Finally, Tukey's test for pairwise comparison of means was used in order to determine the trends of the samples that exhibited different behaviour. The level of significance of $p<0.05$ was chosen. The statistical analysis was performed using Minitab 17 statistical package (Minitab Inc., PA, US).

3 Results and Discussion

3.1 Preparation and characterisation of whey protein fluid gels

Whey proteins upon heating undergo an irreversible denaturation, which takes place in a two-step mechanism. First the globular protein species present in whey (predominately β-lactoglobulin and α-lactalbumin) unfold, exposing many of their active groups. On a second step, these exposed groups form covalent bonds causing the proteins to aggregate and form a 3-dimensional network (Mulvihill & Donovan, 1987). When heat denaturation occurs at pH higher or lower than the isoelectric point the resulting aggregates have a fibrilar shape and appear clear. On the other hand when denaturation happens close to the isoelectric point (around 4.9 for whey) the aggregates have a more compact spherical shape and appear opaque (Schmitt, Bovay, Rouvet, Shojaei-Rami, & Kolodziejczyk, 2007). The presence of electrostatic interactions therefore, seems to be detrimental for the structure of these aggregates. In order for whey proteins to form a gel, a set of conditions has to be met. For the given environmental conditions (pH and ionic strength) there is a critical protein concentration (C_g) and a critical temperature (T_g) needed in order to form a gel. Generally both C_g and

211 T_g increase while moving away from the isoelectric point. At pH 8 the critical
212 concentration is approximately 12 wt% and the critical temperature is 80 ºC, when heat
213 is provided with a rate of 1 ºC min^{-1} (Stading & Hermansson, 1990).

214 During the heat gelation of whey proteins under shear, nuclei are formed as a
215 consequence of the disruption to the secondary structure, which leads to the formation
216 of oligomers. These nuclei grow through a series of weak interactions and covalent
217 bridging up to an aggregate size, which is limited by the magnitude of the shear applied.
218 Subsequently, the disruption of the shear intra particle interactions can cause bridging
219 mainly due to disulphide bonds, which lead to the formation of a continuous network. A
220 way of manipulating the size of the aggregates formed is by choosing the magnitude of
221 the applied shear and the heating rate. It has been shown that at large shear rates
222 (higher than 600 s^{-1}) the size of the aggregates is limited by the shear whilst at lower
223 shear rates the size of the aggregates is generally larger but can be retained by
224 choosing lower heating rates (Fernández Farrés, Moakes, & Norton, 2014).

225 The kinetics of the fluid gel formation can be monitored by applying a uniform shear
226 within the geometry of a rheometer while a heating profile is being administered. In this
227 study the viscosity profile during the formation of whey protein fluid gels at a protein
228 concentration of 12 wt% at pH 5 and pH 8 with a heating rate of 3 ºC min^{-1} were
229 monitored within the flow field of a vane geometry (Figure 2). For both systems there is a
230 notable increase in viscosity when the temperature reaches 80 ºC which indicates the
231 beginning of gelation. This increase continues until it reaches a maximum, suggesting
232 the end of gelation. Both the maximum viscosity (0.9 Pa s) and the time needed for it to
233 be attained seems to be independent of the pH. Upon cooling, the fluid gels made at pH
234 8 retain their high viscosity whilst the fluid gels made at pH 5 show a dramatic drop in
235 viscosity. The high viscosity sustained at pH 8, even though the shear environment is

236 still present, suggests that the structure and interaction between the aggregates created
237 remain unchanged. On the other hand, the drop in viscosity at pH 5 indicates that the
238 size of the aggregates continues to decrease under shear, as there are limited
239 interactions between the aggregates.

240 The fact that the gelation starts and ends at the same time at the given concentration
241 and heating rate for the systems at the two different pH values implies that the
242 conditions for gelling are the same and therefore the two systems can be created under
243 the same conditions. When fluid gels were prepared inside the geometry of the
244 rheometer, the sample was exposed to the atmosphere allowing the incorporation of air
245 and limited foaming occurred during the preparation of the fluid gel which to an extend
246 added to the increase of the values of viscosity. This phenomenon was more profound in
247 the fluid gel samples made at pH 8 which can have also partially contributed to the
248 retention of the initial viscosity. Finally the fluid gels made at pH 8 tend to post-order
249 during cold storage and form a non-flowable gel. This is believed to happen due the
250 larger number of available -SH groups in gel structures created at elevated pH values
251 which can form S-S bridges over time and cause the system to form a continuous
252 network (Klemaszewski & Kinsella, 1991). Post ordering was prevented by diluting the
253 fluid gels at the desired concentrations (1, 3 and 5 wt%) right after their production. The
254 reduction in the packing of the gel particles did not promote the formation of significant
255 amount of disulphide bridges and the fluid gels remained flowable without their viscosity
256 increasing over time.

257 The main purpose of this study was to create WPI fluid gels in a continuous manner.
258 In terms with this, the production of fluid gels was done as described in Section 2.1 in a
259 pin stirrer device for both systems at pH 5 and pH 8. The production set up did not allow
260 the application of as wide a range of shear or heating rates as could have been achieved

261 within a rheometer. According to a series of computational fluid dynamic (CFD)
262 calculations carried out on a pin stirrer device with the same geometry the maximum
263 shear rate is behind the rotating pins at a rotational speed of 2000 rpm and is in the
264 order of 200 s^{-1} (Gabriele, 2011). The effect of the rotation speed of the pin stirrer (500 to
265 2000 rpm) and the heating rate (2 to 6 ºC min^{-1}) within the limits allowed by the system
266 did not have a significant impact on the size of the particles present in the fluid gels (data
267 not shown here).

268 The size of the gel particles obtained from this production method is significantly
269 dependent on the pH at which the fluid gels were made as shown in Figure 3. The size
270 of the aggregates at pH 5 is significantly smaller with a $D_{3,2}$ around 10 µm, whilst the
271 samples produced at pH 8 consisted of larger sized aggregates of approximately 150
272 µm. This is due to the fact that at pH 5 the fluid gels exist as compact spherical
273 aggregates with a structure at the particle level resembling that of quiescent gels made
274 at the same conditions in the absence of shear (Figure 4a) (Schmitt et al., 2014). On the
275 other hand, at pH 8 whey proteins tend to create fibrillar aggregates which when formed
276 in the presence of shear seem to create larger but still spherical structures as shown in
277 Figure 4c. The transparency of the fluid gels produced at pH 8 is caused by the similarity
278 of the refractive index of the gel particles with that of the continuous aqueous phase
279 which makes distinguishing them microscopically, but also in terms of dynamic laser
280 scattering, difficult. No increase in size was observed after the adjustment of the pH of
281 the fluid gels that were prepared at pH 5 to 8. The properties of these pH-adjusted
282 samples have also been investigated in this study and are referred to as pH 5 adj. to 8
283 throughout this work.

284 Proteins are charged species and many of their functional properties depend on the
285 level of charge and the electrostatic interactions caused as a result of this. The effect,

286 therefore, of the pH on the charge in terms of ζ-potential of these systems is of
287 importance and was investigated. The ζ-potential over a wide range of pH values (pH 2
288 to 12) of dilute WPI fluid gel dispersions made at pH 5 and pH 8 and compared with
289 native WPI showed a shift to the original isoelectric point (4.8) (Figure 5). The fluid gels
290 made at pH 8 show a lower isoelectric point closer to 4.1 whilst the fluid gels made at pH
291 5 show an isoelectric point similar to that of native proteins. Moreover, differences in ζ-
292 potential behaviour can be observed at the pH values between pH 5 and 8. The fluid
293 gels made at pH 8 show higher levels of charge than the ones prepared at pH 5 and the
294 native proteins. This difference is not as prominent at pH higher than 8 and lower than 4.
295 The shown differences in ζ-potential suggest also changes to the magnitude of the
296 electrostatic repulsions between particles in these systems, even at the same pH. This
297 dependence of the pH at which the fluid gels were made on the electric charge of the
298 system can be due to the difference in the amount of free non-aggregated proteins still
299 present in the system following the heating step. Recent work (unpublished) by the
300 authors has shown that the amount of non-aggregated proteins in the system is higher
301 when the gelation takes place at pH 5 compared to pH 8.

302 ## 3.2 Interfacial properties of WPI fluid gels

303 The functional properties of proteins also depend on their ability to adsorb at
304 surfaces/interfaces and lower the surface/interfacial tension of the system stabilising the
305 newly formed interface. This behaviour is important when looking at colloidal systems
306 such as foams, where the surface tension (SFT) of the system is a good indicator of the
307 ability of the surfactants, in this case proteins, to adsorb on the interface during foaming.
308 When statistically comparing the SFT values (Table 1) of the samples it seems that the
309 samples made at pH 5 and then readjusted to 8 and the heat treated WPI have
310 significantly lower values which is also dependant on the concentration. Whilst the

311 samples made at pH 8 and at pH 5 have higher values. It is worth mentioning that the
312 difference between the lowest (heated WPI 5 wt%) and highest (WPI FG pH 5 1 wt%)
313 mean is less than 4 mN/m^2. Therefore there might be statistical differences between the
314 samples but these are in reality small. This indicates that the ability of the protein
315 systems to lower the surface tension remains unaffected by exposure to heat during fluid
316 gel production. This is probably due the presence of a significant amount of non-
317 aggregated proteins, which rapidly adsorb and saturate the surface across all samples
318 studied, but also due to the ability of the formed protein aggregates to adsorb on the a/w
319 interface. The WPI fluid gels contain enough protein material that can diffuse fast and
320 adsorb on the interface lowering the surface tension and allowing the formation of a
321 foam.

322 Colloidal particles have shown to stabilise foams due to their ability to adsorb on the
323 air/water interface and form a strong film (Dickinson & Murray, 2006). The strength of
324 this film provides an energy barrier that prevents the diffusion of gas between different
325 sized bubbles (disproportionation). During disproportionation the bubbles tend to shrink
326 and in order for that to happen the bubbles have to work against the interfacial elasticity
327 and viscosity which can suppress shrinkage (Murray & Ettelaie, 2004). When particles
328 adsorb at the air/water interface the resulting increase in interfacial elasticity and
329 viscosity reduces significantly the diffusion of gas between bubbles of different size and
330 therefore disproportionation. The interfacial rheological properties of the systems studied
331 here were therefore investigated using pedant drop tensiometry. The interfacial elasticity
332 and viscosity values of native and heated WPI were also measured for means of
333 comparison as shown on Table 1.

334 The conventional condition that bubbles are stale against disproportionation is the
335 Gibbs stability criterion in Equation 5 (Martinez et al., 2008). The surface elasticity and

viscosity values of the control systems (native and pre-heated WPI) show a maximum at 3 wt% concentration indicating that at this level the packing at the interface is optimum giving the highest film strength. The WPI fluid gels produced at pH 5 showed a statistically significant decrease in both surface elasticity and viscosity compared to the control systems indicating that the Gibbs criterion is not met.

$$E' > \frac{\sigma_{a/w}}{2} \quad (5)$$

When the pH of the same fluid gels was adjusted to 8 then both the surface elasticity and viscosity increased significantly (statistically not different to the control systems for the 5 wt% concentration). The fluid gels produced at pH 8 had higher values of interfacial elasticity and viscosity than the ones at pH 5 and statistically similar to the ones when the pH was readjusted from 5 to 8. This implies that both electrostatic repulsions and size affect the interfacial rheological properties of these systems. More specifically the interfacial elasticity increases enough to fulfil that $E' > \sigma_{a/w}/2$, implying that disproportionation can be significantly limited. The smaller gel particles produced at pH 5 when provided with a charge by increasing the pH to 8 can produce films that have high elasticity and viscosity but not higher than the ones of native or heat treated proteins. This is either due to weak adsorption of these particles on the interface or lack of complete interfacial coverage.

3.3 Bulk rheological properties

The viscosity of the bulk phase affects the mobility of the continuous phase around the foam bubbles and therefore influences the rate of foam drainage (Yang & Foegeding, 2011). Investigating the effect of the pH on the viscosities of the different WPI fluid gels and comparing with those of native WPI at the same concentrations

359 revealed an overall increase in the fluid gel viscosity, especially at the higher
360 concentrations studied (3 and 5 wt%).

361 All samples show a shear thinning behaviour that suggests the presence of
362 interactions and structural formation, which eventually disrupted by shear (Figure 6a).
363 The fluid gels made at pH 5 show the lowest viscosity values amongst the fluid gel
364 samples but when their pH is adjusted to 8 there is a clear increase in shear viscosity.
365 This indicates that the introduction of pH-induced electrostatic repulsions amongst the
366 protein species and fluid gel particles is causing the viscosity to increase. The fluid gels
367 produced at pH 8 have the significantly highest viscosity especially at the 5 wt%
368 concentration studied (Figure 6b). This is most certainly due to the larger particles
369 present in combination with the higher magnitude of electrostatic forces as suggested by
370 the higher ζ-potential values.

371 The liquid/solid behaviour of the WPI fluid gels has been studied through
372 measurements of the storage and loss moduli from the viscoelastic response to
373 oscillations within the linear viscoelastic region (Figure 7). The WPI fluid gels produced
374 at pH 5 exhibit significantly low values for both storage and loss moduli showing a liquid
375 behaviour. When the pH of the same sample was increased to pH 8 both elasticity and
376 viscosity increased. The elasticity values increased for all concentrations and a weak gel
377 behaviour could be observed for the sample at 5 wt% at the lower frequencies were both
378 G' and G" are close to each other and remain parallel. The fluid gels produced at pH 8
379 showed intermediate values for both G' and G" across all concentrations studied but not
380 statistically different from the ones made at pH 5 and then adjusted to 8. Additionally, at
381 5 wt% an elastic solid to viscous liquid transition at high frequencies was observed as
382 suggested by a cross over of the G' and G" curves. The combination of aggregate size
383 and level of electrostatic repulsions appear to affect the elasticity of WPI fluid gels

indicating that both the pH at which they are made but present plays an important role in their viscoelastic response.

3.4 Foaming properties of WPI fluid gels

The functionality of WPI fluid gel systems in terms of producing and stabilising foams is presented here. The ability of the fluid gels to incorporate sufficient amount of air and produce foams was assessed in terms of overrun (Table 1). All fluid gel samples were able to produce foams with very similar overrun to the ones made by native proteins. The statistical evaluation has shown that the fluid gel samples made at pH 8 and pH 5 produced foams with the highest overrun values amongst the samples studied but still with values close to the native proteins. The ability of the system to incorporate air was not hindered as it is common with particle containing systems (Murray & Ettelaie, 2004). The overrun results are in agreement with the surface tension data (Table 1) indicating that for all fluid gel systems the controlling factor is the sufficient amount of soluble proteins that can diffuse fast to the newly formed interface and stabilise it during the incorporation of air to the system.

The stability of the foams produced by the WPI fluid gel systems was evaluated in terms of foam half-life (Figure 8). The fluid gel systems showed similar foam stabilising behaviour to systems containing dried gel protein particles and an overall significant increase in foam stability compared to native WPI was observed for all samples (Lazidis et al., 2014). Whilst the error bars representing the standard deviation between at least 4 replicates appear quite large due to the nature of the measurement, the foam stability of the systems can be illustrated. The fluid gels produced at pH 5 while only moderately increase the stability of protein foams at their intrinsic pH showed statistically significant increase in foam stability once their pH was increased to pH 8 especially at 3 and 5 wt% concentrations, the highest amongst all samples. Fluid gels produced at pH 8 were also

409 able to produce foams with increased stability (compared to those stabilised by native
410 proteins) but did not perform as well as the fluid gels of smaller aggregate size (formed
411 at pH 5 and adjusted to pH 8) even though the charge was smaller as indicated by the ζ-
412 potential data. The importance of size was therefore highlighted as the most important
413 factor affecting foam stability followed by the existence and the extent of electrostatic
414 repulsions. Foam stability displayed a maximum value for the 3 wt% protein
415 concentration fluid gels showing that further increase in protein concentration had limited
416 effect within the range studied.

417 The effect of the pH at which the WPI fluid gels were formed and their concentration
418 on the rate of drainage of the foams these stabilised was also investigated. The rate of
419 drainage was determined by measuring the electric conductivity of the foam and
420 calculating the amount of water present in the foam over time (section 2.4). In all
421 samples the majority of liquid drainage took place within the first 10 minutes after foam
422 formation. As shown in Figure 9, the liquid drainage is affected by both the pH at which
423 the fluid gel system was formed and then adjusted at, and by the overall protein
424 concentration. Foam drainage behaviour follows closely that observed from foam half-life
425 data. The fastest drainage was observed in the foams stabilised by WPI fluid gels
426 formed at pH 5 and aerated at their intrinsic pH. On the other hand when the fluid gel pH
427 was increased to pH 8 (following formation and before aeration) drainage was
428 significantly reduced especially for the higher protein concentration fluid gels studied.
429 This indicates that while non-charged small spherical fluid gels although they do position
430 themselves around air bubbles do not prevent the flow of the continuous phase due to
431 gravity. When the same fluid gel structures are adjusted to pH 8 and the aerated,
432 drainage is reduced potentially by the increase in the local (around the air bubbles)
433 rheology as demonstrated through the oscillatory rheology data. Foams stabilised by

fluid gels made at pH 8 showed a moderate rate of drainage probably due to their larger size which potentially causes them to be excluded from the spaces between the bubbles which did not seem to be the case with the smaller aggregates.

The microstructure of foams stabilised by the different WPI fluid gels structures were also visualised by confocal laser scanning microscopy (CLSM). Images taken from foams stabilised by these systems show that in the case of the fluid gels formed at pH 5 (Figure 10a) were the aggregates are smaller and spherical seem to occupy some of the space around the bubbles and potentially adsorb on the air water interface and partially cover it. The partial coverage of the bubbles was also present after increasing the pH of those systems to 8 (Figure 10b) indicating that it is not dependent on the presence of charge. In the case of the foams stabilised by the fluid gels formed at pH 8 there seems to be exclusion of the particulates from the space between the air bubbles.

4 Conclusions

WPI fluid gels produced by thermally treating WPI under shear show interesting foaming properties which are dependent on both the pH at which these structures were originally formed but also the pH at which they were aerated.

Fluid gels made at pH 5 whilst not having any specific foaming functionality at their intrinsic pH, when adjusted and aerated at pH 8, demonstrated an enhanced foaming capacity. This is due to what is proposed as an enhancement to the electrostatic inter-particle interactions promoted by the change to the pH environment. This is supported by both the ζ-potential measurements but also by the presented interfacial elasticity and viscosity data. The small aggregates formed at pH 5 seem to be able to fill effectively the spaces between the bubbles and reduce the rate of liquid drainage by the particles

457 acting as corks anchored on the interface and increase the local viscosity around the
458 bubbles improving the stability of foams.

459 Fluid gels formed at pH 8, while having stronger charge and higher bulk viscosity and
460 elasticity were able to produce less viscoelastic films probably due to the larger size of
461 the aggregates present, which limited their ability to pack which lead to exclusion from
462 the spaces around the air bubbles. This resulted in producing stable foams compared to
463 native proteins by reducing the rate of liquid drainage but not to the same extent as the
464 fluid gels made at pH 5 and aerated after adjustment to pH 8.

465 Acknowledgements

466 We thank Dr. Bettina Wolf and Dr. Amelia Torcello Gomez from the Food Science
467 Department of the University of Nottingham for the use of the pendant drop tensiometer
468 in their laboratory. The help of Dr. Hani El Kadri in setting up the logging system of the
469 foam conductivity apparatus is appreciated. The financial support of Nestlé and the
470 Engineering and Physical Sciences Research Council (EPSRC), UK is gratefully
471 acknowledged.

472 References

473 Barigou, M., Deshpande, N. S., & Wiggers, F. N. (2001). An enhanced electrical
474 resistance technique for foam drainage measurement. *Colloids and Surfaces A:*
475 *Physicochemical and Engineering Aspects*, *189*(1–3), 237–246.
476 Brockman, C., & Beeren, C. J. M. (2011). Additives in Dairy Foods | Consumer
477 Perceptions of Additives in Dairy Products. In J. W. Fuquay (Ed.), *Encyclopedia*
478 *of Dairy Sciences (Second Edition)* (pp. 41–48). San Diego: Academic Press.

479 Dickinson, E., & Murray, B. S. (2006). Stabilization of bubbles and foams by adsorbed
480 proteins and nanoparticles. Presented at the 4th International Symposium on
481 Food Rheology and Structure, ETH Zurich.
482 Eric Dickinson. (2010). Food emulsions and foams: Stabilization by particles. *Current*
483 *Opinion in Colloid & Interface Science*, *15*(1-2), 40–49.
484 Fernández Farrés, I., Moakes, R. J. A., & Norton, I. T. (2014). *Designing biopolymer fluid*
485 *gels: A microstructural approach*.
486 Gabriele, A. (2011). *Fluid Gels: formation, production and lubrication* (PhD Thesis).
487 University of Birmingham, Birmingham.
488 Kinsella, J. E. (1981). Functional properties of proteins: Possible relationships between
489 structure and function in foams. *Food Chemistry*, *7*(4), 273–288.
490 Klemaszewski, J. L., & Kinsella, J. E. (1991). Sulfitolysis of whey proteins: effects on
491 emulsion properties. *Journal of Agricultural and Food Chemistry*, *39*(6), 1033–
492 1036.
493 Lazidis, A., Hancocks, R. D., Spyropoulos, F., Kreuß, M., Berrocal, R., & Norton, I. T.
494 (2014). Stabilisation of foams by whey protein gel particles (pp. 252–262).
495 Presented at the Gums and Stabilisers for the Food Industry 17 - The Changing
496 Face of Food Manufacture: The Role of Hydrocolloids.
497 Martinez, A. C., Rio, E., Delon, G., Saint-Jalmes, A., Langevin, D., & Binks, B. P. (2008).
498 On the origin of the remarkable stability of aqueous foams stabilised by
499 nanoparticles: link with microscopic surface properties. *Soft Matter*, *4*(7), 1531–
500 1535.
501 Mulvihill, D. M., & Donovan, M. (1987). Whey Proteins and Their Thermal Denaturation -
502 A Review. *Irish Journal of Food Science and Technology*, *11*(1), 43–75.

503 Murray, B. S., Durga, K., Yusoff, A., & Stoyanov, S. D. (2011). Stabilization of foams and
504 emulsions by mixtures of surface active food-grade particles and proteins. *Food*
505 *Hydrocolloids*, *25*(4), 627–638.
506 Murray, B. S., & Ettelaie, R. (2004). Foam stability: proteins and nanoparticles. *Current*
507 *Opinion in Colloid & Interface Science*, *9*, 314–320.
508 Norton, I. ., Jarvis, D. ., & Foster, T. . (1999). A molecular model for the formation and
509 properties of fluid gels. *International Journal of Biological Macromolecules*, *26*(4),
510 255–261.
511 Rullier, B., Novales, B., & Axelos, M. A. V. (2008). Effect of protein aggregates on
512 foaming properties of β-lactoglobulin. *Colloids and Surfaces A: Physicochemical*
513 *and Engineering Aspects*, *330*, 96–102.
514 Schmitt, C., Bovay, C., & Rouvet, M. (2014). Bulk self-aggregation drives foam
515 stabilization properties of whey protein microgels. *Food Hydrocolloids*.
516 Schmitt, C., Bovay, C., Rouvet, M., Shojaei-Rami, S., & Kolodziejczyk, E. (2007). Whey
517 Protein Soluble Aggregates from Heating with NaCl: Physicochemical,
518 Interfacial, and Foaming Properties. *Langmuir*, *23*(8), 4155–4166.
519 Stading, M., & Hermansson, A.-M. (1990). Viscoelastic behaviour of β-lactoglobulin gel
520 structures. *Food Hydrocolloids*, *4*(2), 121–135.
521 Walstra, P. (2003). *Physical chemistry of foods*. CRC Press.
522 Waniska, R. D., & Kinsella, J. E. (1979). Foaming Properties of Proteins: Evaluation of a
523 Column Aeration Apparatus Using Ovalbumin. *Journal of Food Science*, *44*(5),
524 1398–1402.
525 Yang, X., & Foegeding, E. A. (2011). The stability and physical properties of egg white
526 and whey protein foams explained based on microstructure and interfacial
527 properties. *Food Hydrocolloids*, *25*(7), 1687–1701.

528 Zhu, H., & Damodaran, S. (1994). Heat-Induced Conformational Changes in Whey
529 Protein Isolate and Its Relation to Foaming Properties. *J. Agric. Food Chem.*,
530 *42*(4), 846–855.
531

Table 1 Interfacial properties of fluid gels and native WPI samples.

Figure 1 Voltage measured through the foam corresponding to the liquid fraction of the foam. Data was fitted with a logarithmic equation with a R^2 value of 0.94

Figure 2 Typical viscosity curve during the production of whey protein fluid gels at 12 wt%

Figure 3 Particle size distributions of protein gel particles present in the fluid gel samples.

Figure 4 Optical microscopy images of WPI Fluid Gels made at pH 5 (a) and (b) and pH 8 (c) and (d).

Figure 5 ζ-potential of the samples over a range of pH.

Figure 6 Flow curves of fluid gels and native WPI at 5 wt% over shear rate (a) and viscosity over protein concentration at 1 s^{-1} (b).

Figure 7 Storage (G') and loss (G") moduli over frequency (error bars were omitted for means of clarity) at 5 wt% (a) and storage moduli (G') at 1 HZ over protein concentration (b).

Figure 8 Half life of the different systems over protein concentration.

Figure 9 Variation of volume of liquid present in foams stabilised by different WPI fluid gel systems at different concentrations over time.

Figure 10 Confocal images of WPI Fluid Gels made at pH 5 (a) pH 5 and adjusted to pH 8 (b) and pH 8 (c), protein aggregates are stained with a fluorescent probe and appear green.

Sample	Protein content	Surface tension after 1200 s (mN m^{-1})	Interfacial elasticity E' (mN m^{-1})	Interfacial viscosity η_d (mN m^{-1} s)	Foam overrun (%)
native WPI	1 wt%	-	41.8 ±7.5	329.7 ±47.2	197.5 ±11.3
	3 wt%		82.5 ±2.1	516.3 ±9.5	205.9 ±19.9
	5 wt%		67.4 ±9.9	454.3 ±35.0	198.9 ±8.3
WPI heated to 80 ºC	1 wt%	49.4 ±0.2	69.3 ±7.2	440.7 ±52.2	-
	3 wt%	50.5 ±0.3	74.6 ±7.4	476.0 ±111.7	
	5 wt%	48.3 ±0.2	54.5 ±1.6	337.1 ±3.0	
pH 5	1 wt%	52.9 ±0.2	13.7 ±0.9	48.4 ±7.7	231.0 ±14.0
	3 wt%	52.6 ±0.6	7.0 ±2.7	10.7 ±9.4	235.2 ±34.8
	5 wt%	51.1 ±0.6	8.9 ±2.7	41.7 ±24.3	212.8 ±8.6
pH 5 adj pH 8	1 wt%	51.6 ±0.6	18.9 ±0.3	142.5 ±60.0	183.4 ±16.9
	3 wt%	50.2 ±0.2	59.4 ±3.2	381.0 ±41.7	207.8 ±16.4
	5 wt%	49.2 ±0.3	55.3 ±10.2	434.3 ±37.3	197.5 ±23.6
pH 8	1 wt%	51.4 ±0.4	51.3 ±8.7	382.5 ±41.0	240.2 ±33.2
	3 wt%	51.8 ±0.1	46.3 ±4.5	266.5 ±14.6	201.0 ±20.6
	5 wt%	51.7 ±0.2	65.9 ±9.3	310.2 ±75.7	241.5 ±25.5

Table 1 Interfacial properties of fluid gels and native WPI samples.

Figure 1 Voltage measured through the foam corresponding to the liquid fraction of the foam. Data was fitted with a logarithmic equation with a R^2 value of 0.94

Figure 2 Typical viscosity curve during the production of whey protein fluid gels at 12 wt%

Figure 3 Particle size distributions of protein gel particles present in the fluid gel samples.

Figure 4 Optical microscopy images of WPI Fluid Gels made at pH 5 (a) and (b) and pH 8 (c) and (d).

Figure 5 ζ-potential of the samples over a range of pH.

Figure 6 Flow curves of fluid gels and native WPI at 5 wt% over shear rate (a) and viscosity over protein concentration at 1 s^{-1} (b).

Figure 7 Storage (G') and loss (G") moduli over frequency (error bars were omitted for means of clarity) at 5 wt% (a) and storage moduli (G') at 1 HZ over protein concentration (b).

Figure 8 Half life of the different systems over protein concentration.

Figure 9 Variation of volume of liquid present in foams stabilised by different WPI fluid gel systems at different concentrations over time.

Figure 10 Confocal images of WPI Fluid Gels made at pH 5 (a) pH 5 and adjusted to pH 8 (b) and pH 8 (c), protein aggregates are stained with a fluorescent probe and appear green.

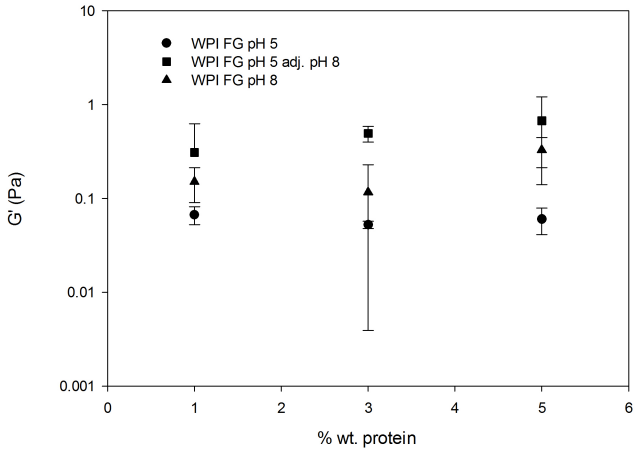

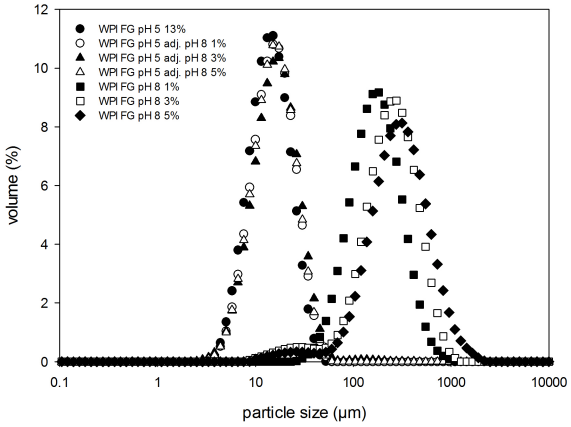

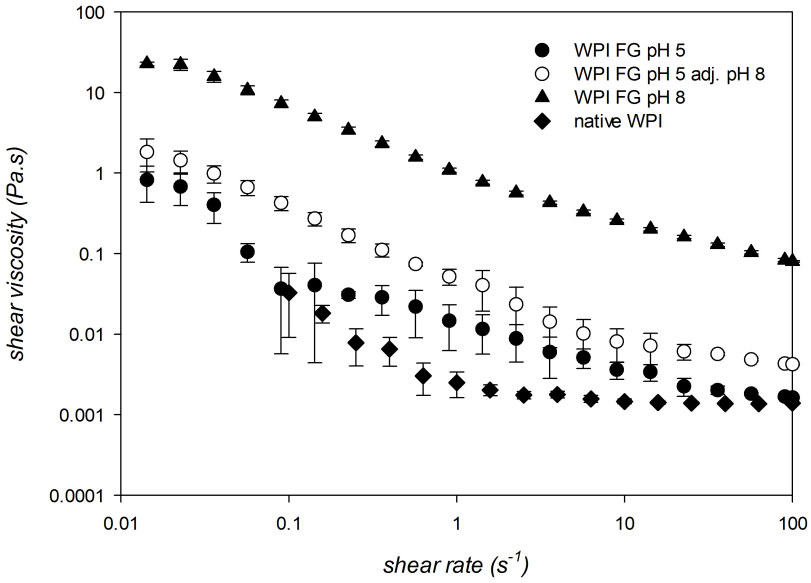

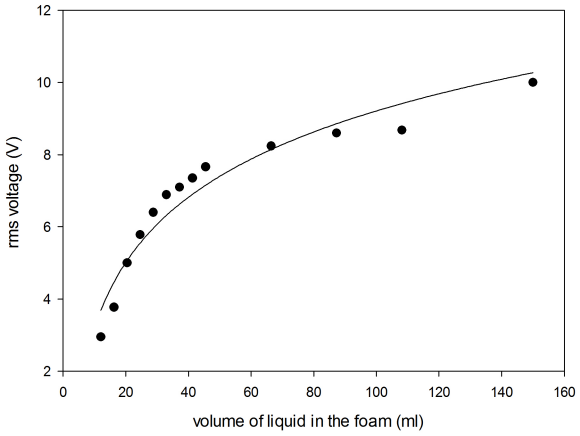

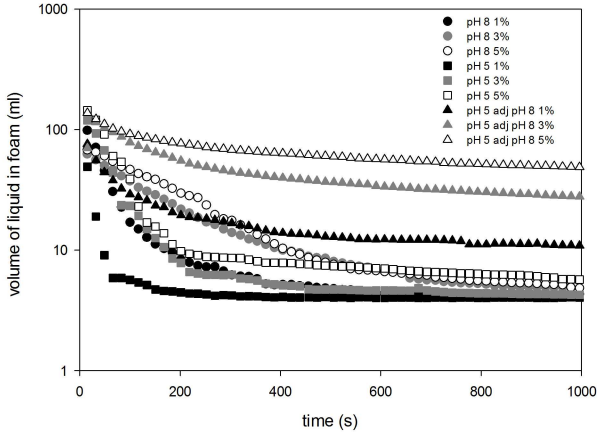

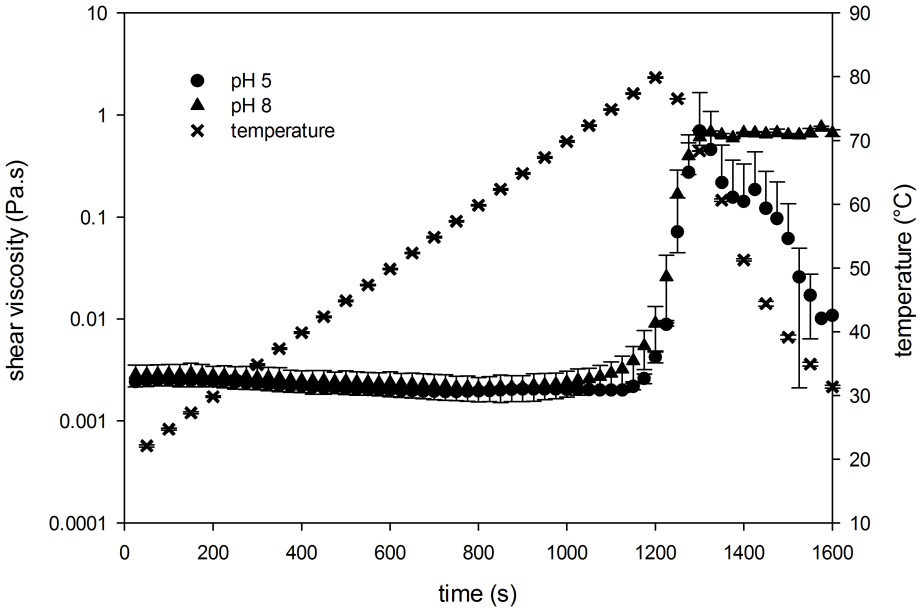
pH 5
pH 8
temperature
shear viscosity (Pa.s)
temperature (°C)
time (s)
10
1
0.1
0.01
0.001
0.0001
90
80
70
60
50
40
30
20
10
0
200
400
600
800
1000
1200
1400
1600

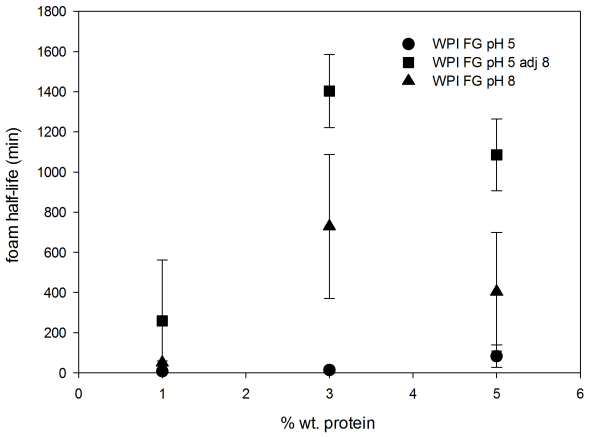

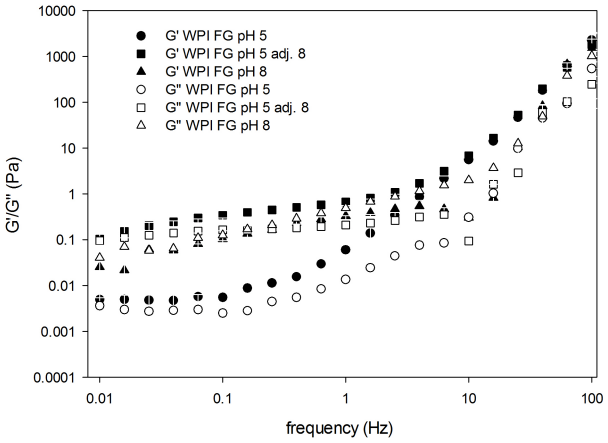

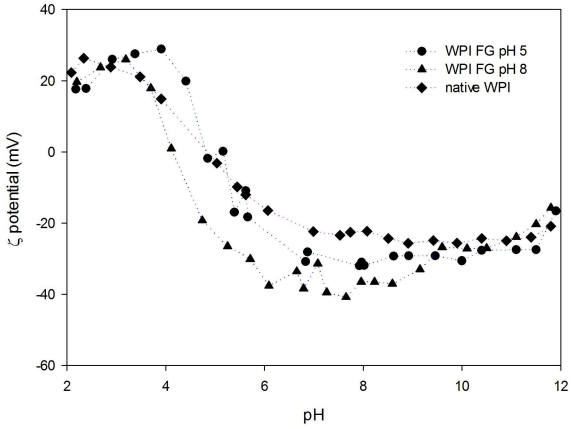

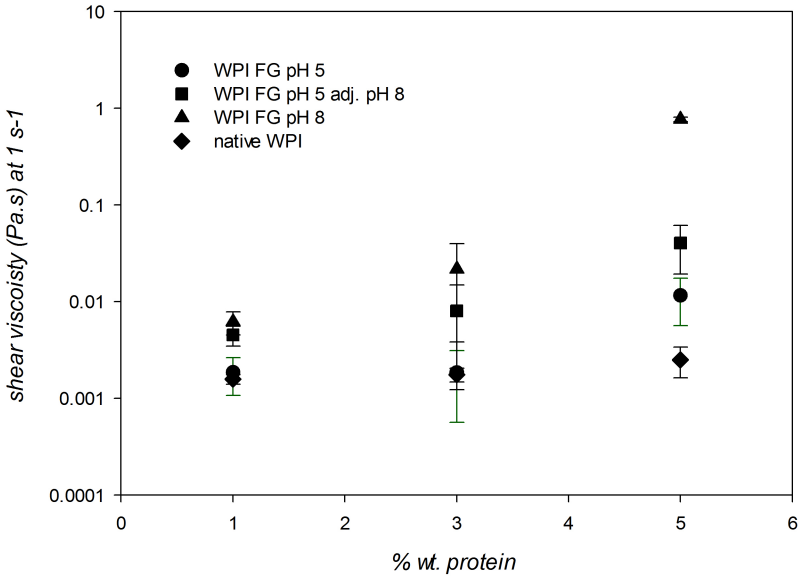
10
1
0.1
0.01
0.001
0.0001
0
1
2
3
4
5
6
shear viscoisty (Pa.s) at 1 s-1
% wt. protein
WPI FG pH 5
WPI FG pH 5 adj. pH 8
WPI FG pH 8
native WPI

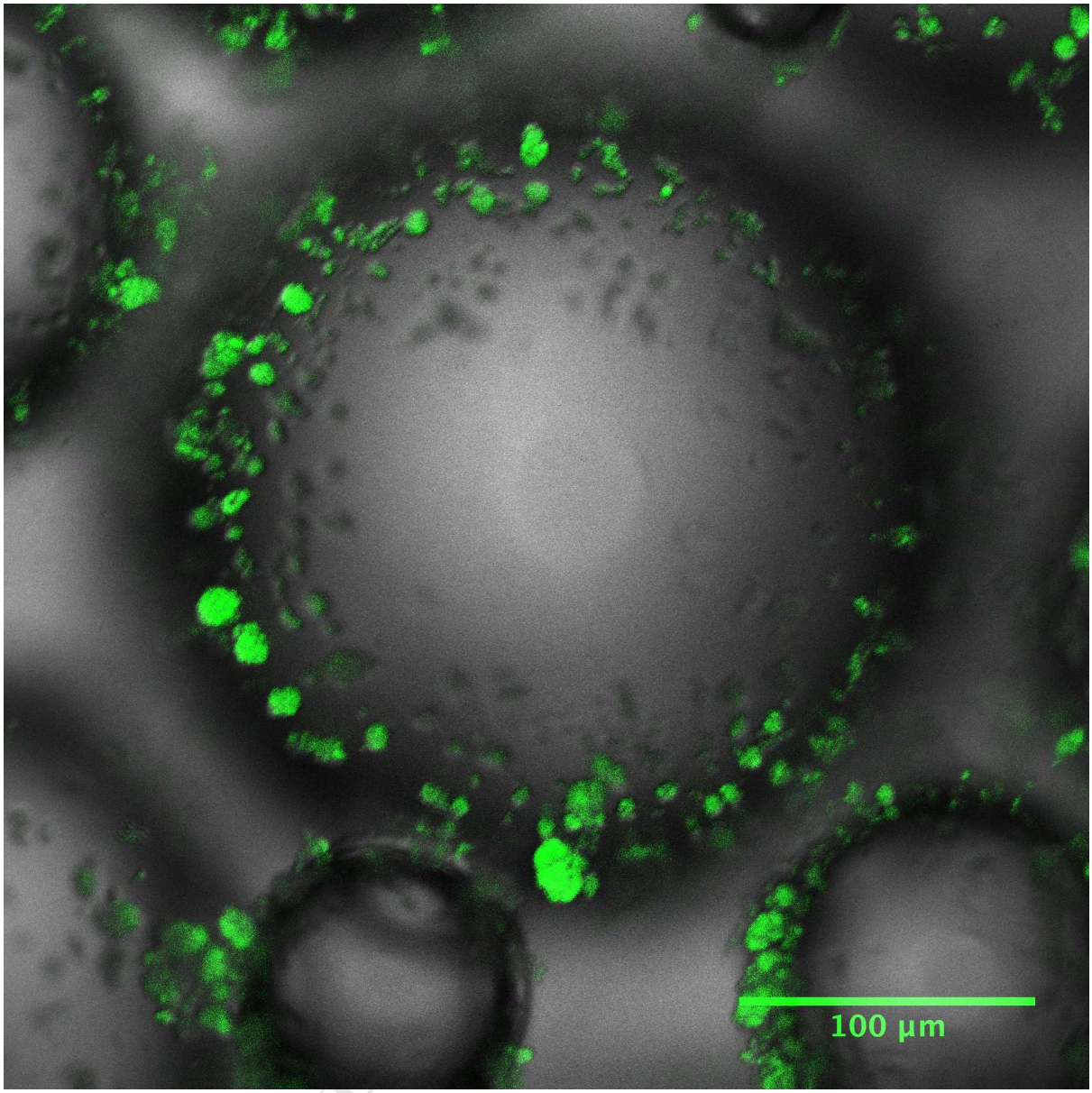

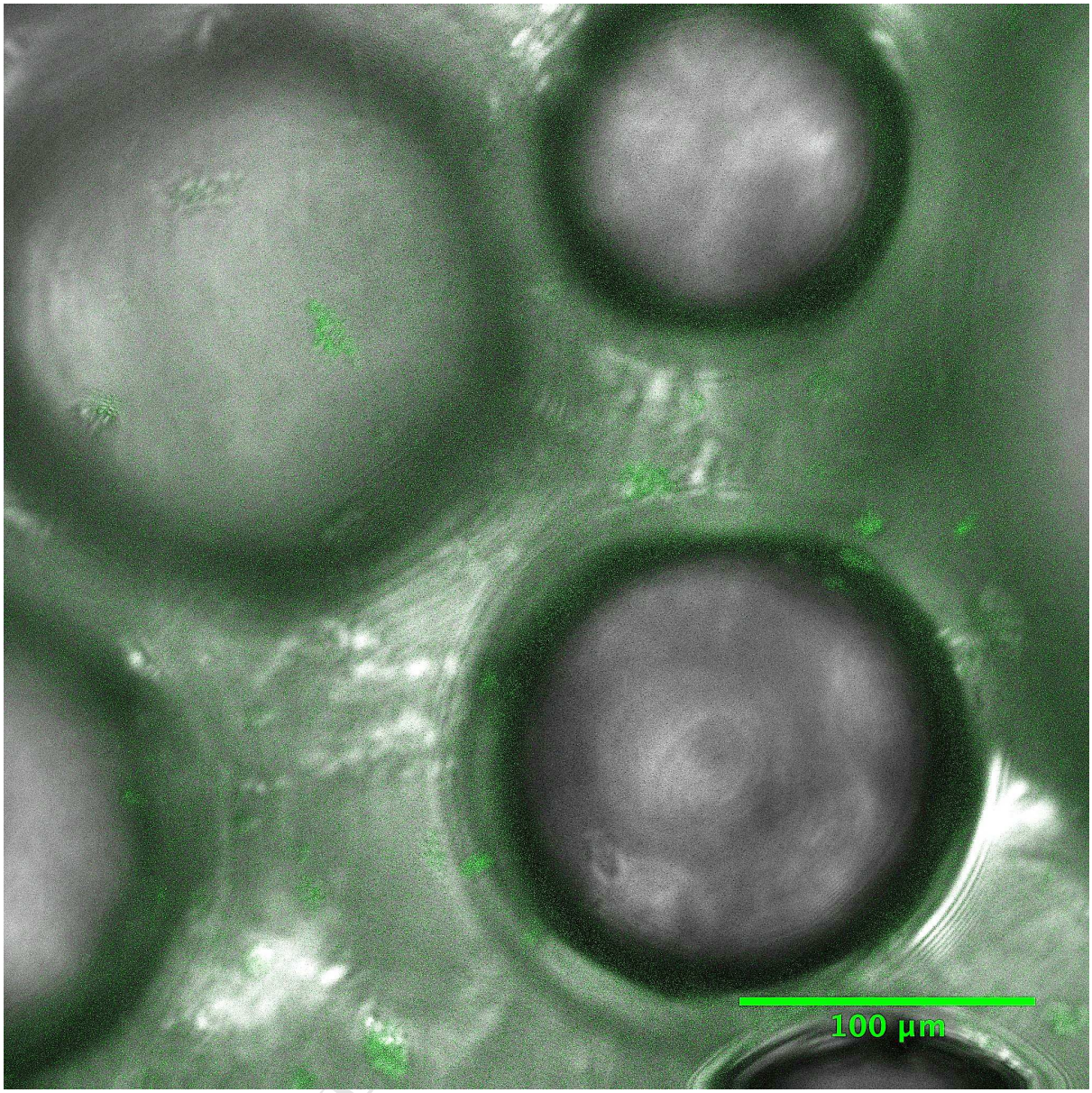

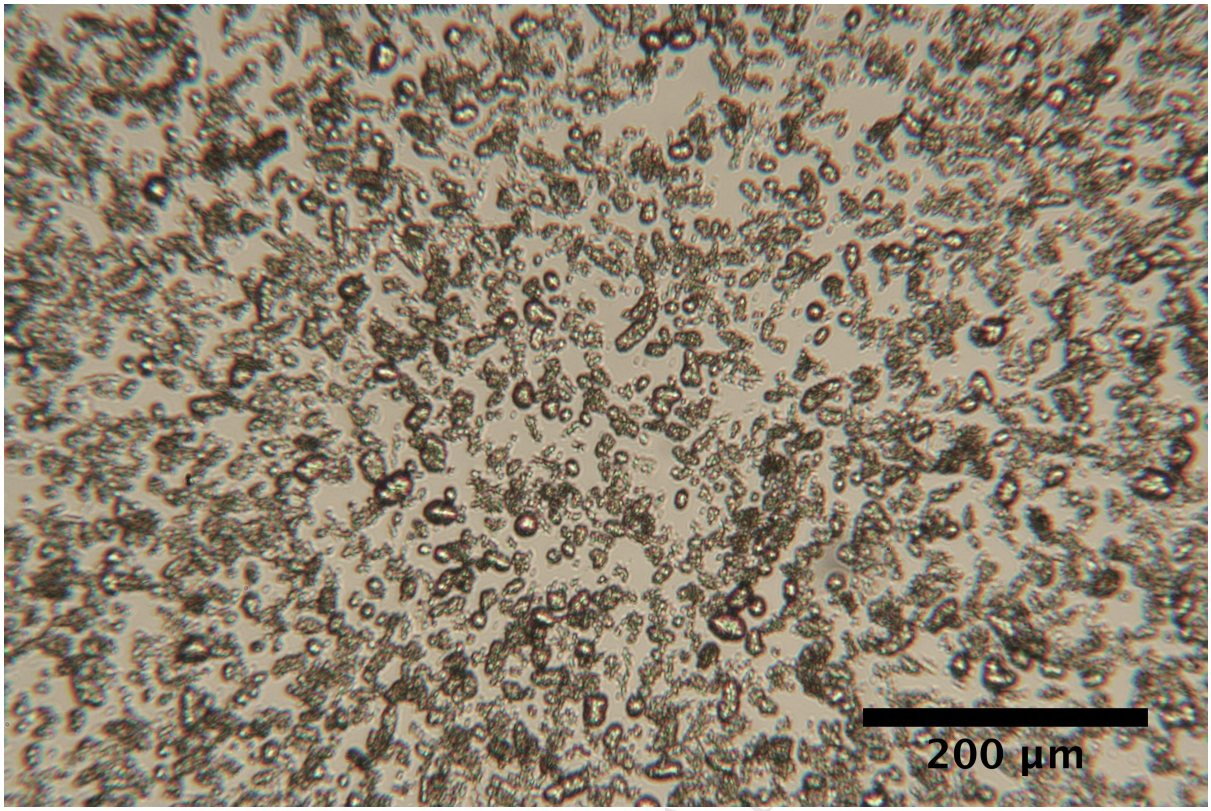

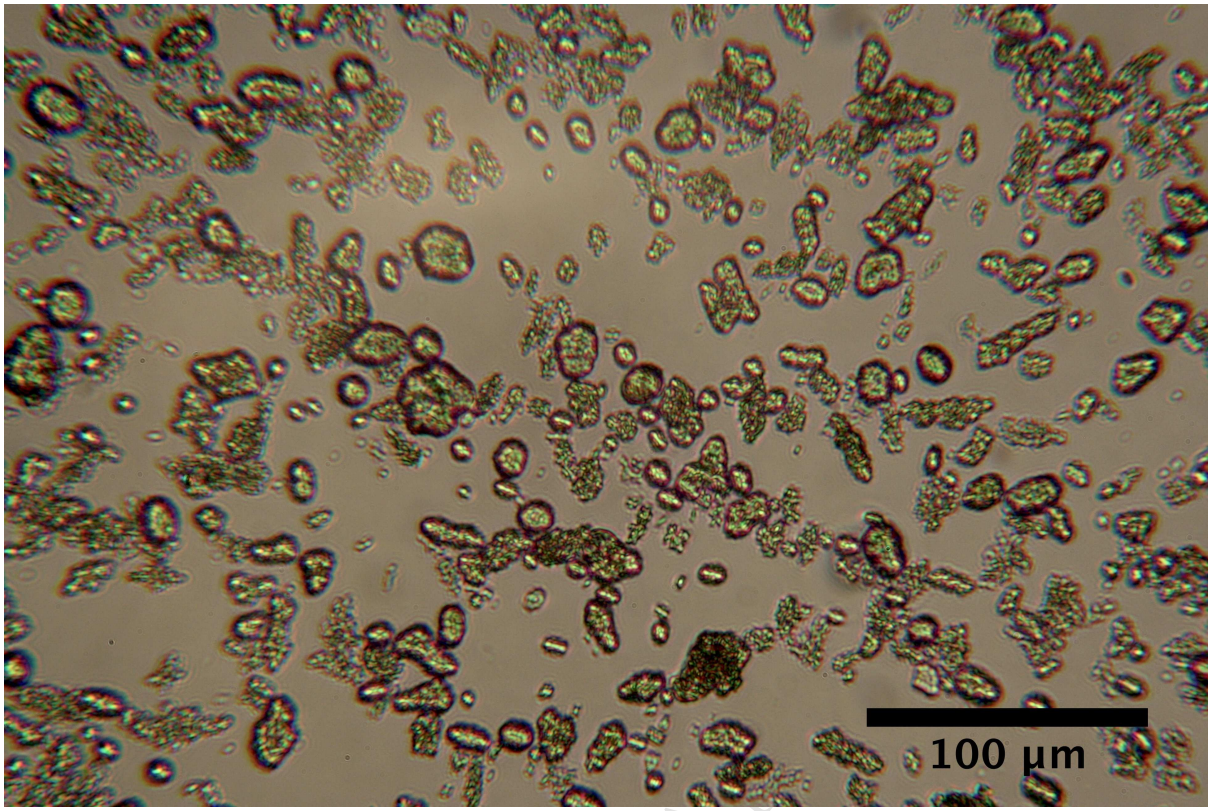

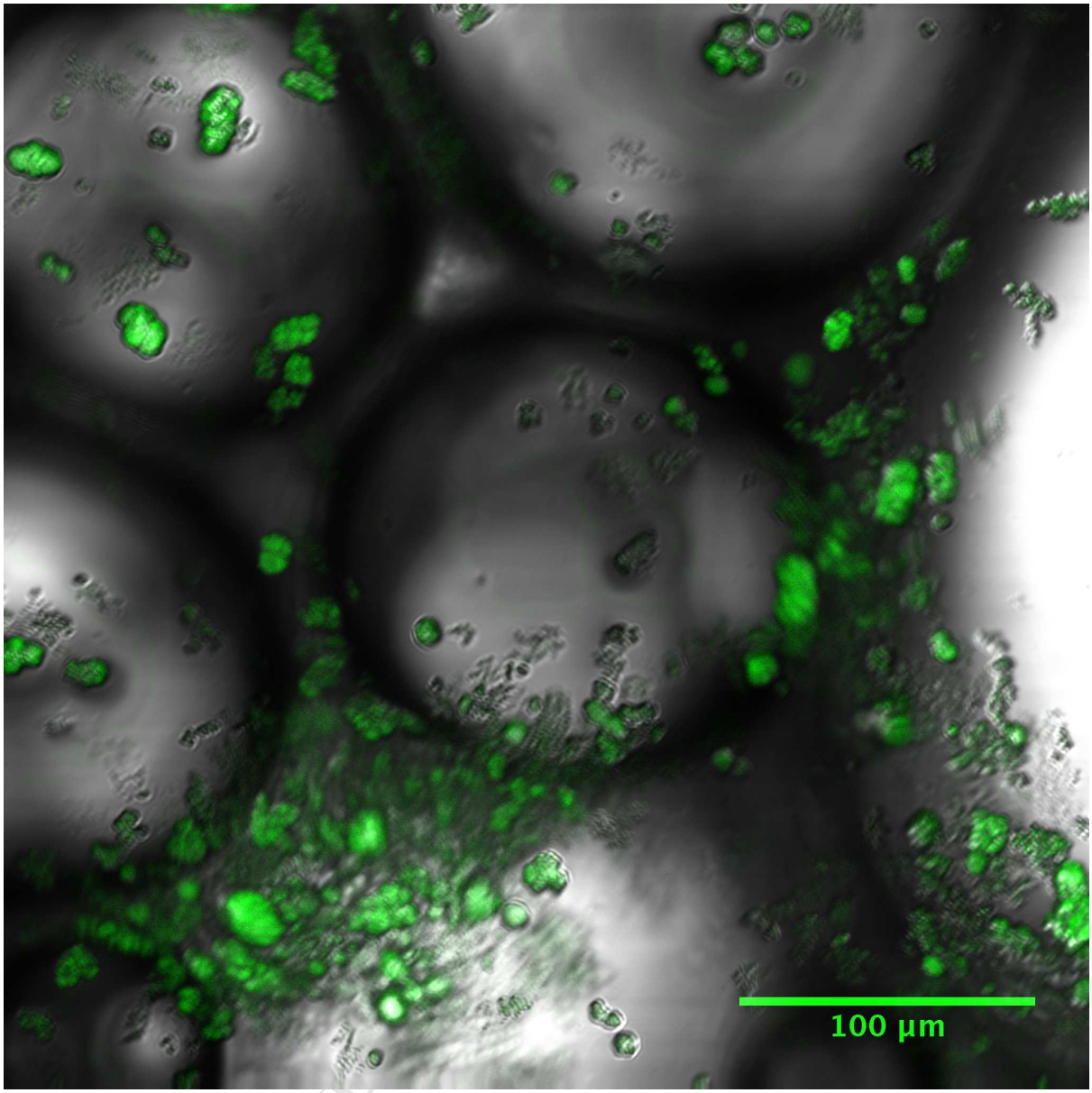

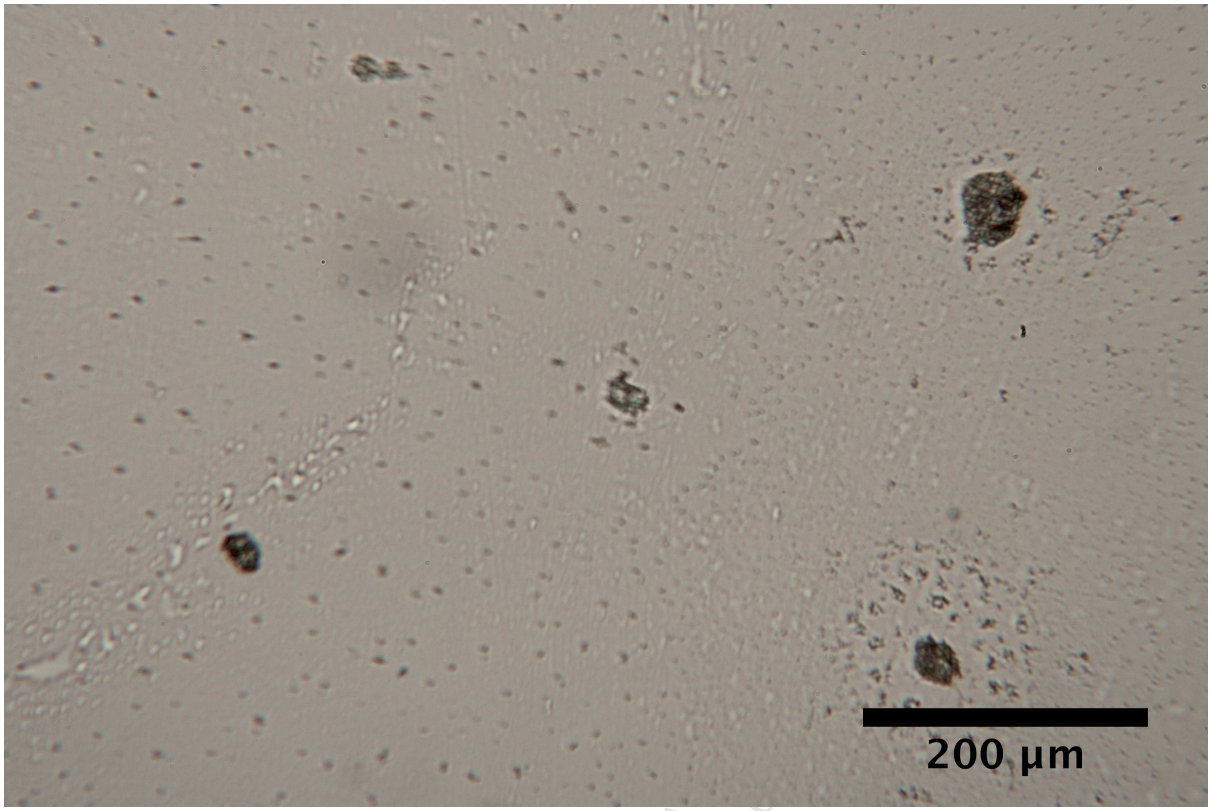

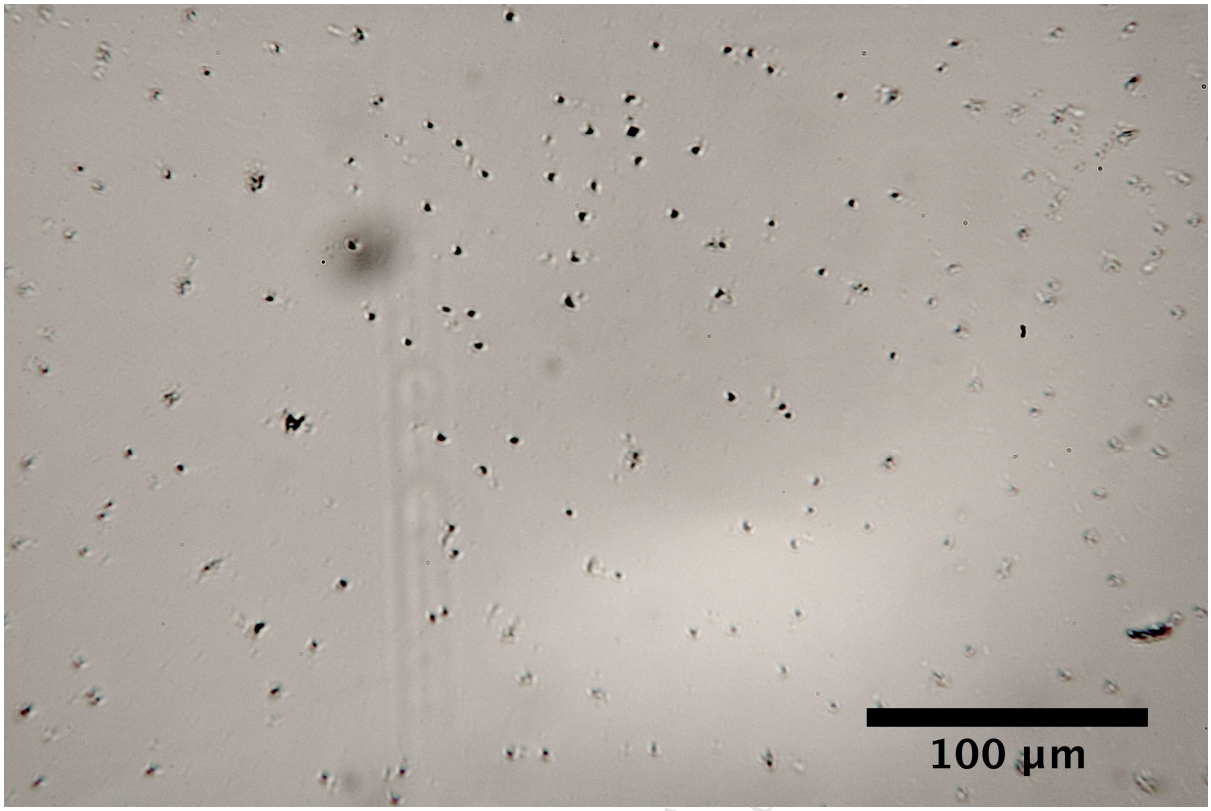

- Whey protein fluid gels were created at pH 5 and pH 8.
- The structure of the aggregates present in the systems was examined.
- The bulk rheological and interfacial properties of the systems were studied.
- The foaming ability and stability of these systems were investigated.
- Whey protein fluid gel systems manufactured at pH 8 produced very stable foams with reduced drainage.